Research Article Vol. 31, No. 3 / 30 Jan 2023 / Optics Express 5002
Optics EXPRESS

Versatile, compact chirped pulse amplifier pump system for ultrafast optical parametric amplifiers

YANNIK ZOBUS,[1,2,*] CHRISTIAN BRABETZ,[2] MARKUS LOESER,[3] DANIEL ALBACH,[3] MATHIAS SIEBOLD,[3] AND VINCENT BAGNOUD[1,2,4]

[1]*Technische Universität Darmstadt, Karolinenplatz 5, 64289 Darmstadt, Germany*
[2]*GSI Helmholtzzentrum für Schwerionenforschung GmbH, Planckstraße 1, 64291 Darmstadt, Germany*
[3]*Helmholtz-Zentrum Dresden - Rossendorf e. V., Bautzner Landstraße 400, 01328 Dresden, Germany*
[4]*Helmholtz-Institut Jena, Fröbelstieg 3, 07743 Jena, Germany*
[*]*y.zobus@gsi.de*

Abstract: We report on the development of a pump system for ultrafast optical parametric amplifiers (uOPA) as an upgrade for the existing uOPA at the Petawatt High Energy Laser for heavy Ion eXperiments (PHELIX) and the new Petawatt ENergy-Efficient Laser for Optical Plasma Experiments (PENELOPE). The system consists of a two-stage chirped pulse amplifier, centered around a high energy Yb:YAG regenerative amplifier that delivers 108 mJ uncompressed output energy, resulting in 92 mJ at 1030 nm after compression, pulse durations of 1.4 ps, a high beam quality of $M^2_{x/y}$ = 1.02 / 1.16 and a relative energy stability of 0.35 %. A second harmonic generation (SHG) efficiency of up to 70 % is achievable and a maximum pulse energy of 43 mJ at 515 nm has been obtained, which is only limited by the damage threshold of the SHG crystal. A self-phase modulation stage makes this system a widely applicable, self-seedable pump module for uOPA without placing strong requirements on its seed oscillator.

1. Introduction

Nowadays, the design of ultrahigh-intensity lasers includes one or several components to help control the temporal profile of short laser pulses. This development has been made necessary because the temporal profile of pulses amplified by chirped-pulse amplification (CPA) [1] exhibits a nanosecond pedestal and pre-pulses, which can damage targets and pre-ionize them in an uncontrolled manner [2]. In the last two decades, this has become an even larger concern because of the increase in laser on-target intensity - recently 10^{23} W/cm^2 were demonstrated [3] - enabled by improvements to the laser technology, which makes experiments more sensitive than before to the temporal background or pre-pulses.

So far, the solution to this problem has consisted in adding one or several modules to the laser system to mitigate the temporal profile degradation happening during amplification. The double CPA concept [4,5], which is based on two CPA amplifiers and an intermediate nonlinear pulse cleaning stage using cross-polarized wave generation (XPW), is a good example of the additional complexity arising from this strategy. In this design, an additional pre-amplifier, a pulse compressor and stretcher are necessary in addition to the XPW-stage. A second widely used solution employs plasma mirrors as pulse-cleaning devices before the interaction point [6,7]. While this technique is well proven, the achievable reduction of the pulse pedestal by 2-3 orders of magnitude comes at the cost of an energy reduction of 20-to-40 % per mirror [8,9] which also has to be replaced regularly.

#477610 https://doi.org/10.1364/OE.477610
Journal © 2023 Received 13 Oct 2022; revised 17 Nov 2022; accepted 18 Nov 2022; published 27 Jan 2023

Optics EXPRESS

As a third option, the direct amplification using ultrafast optical parametric amplification (uOPA) [10,11] keeps the amplifier design relatively simple but it requires a specific pump laser. Contrarily to standard laser amplification, the short pulse pump laser gates the parametric gain over its duration, which is typically of the order of a picosecond. Consequently, no amplification noise takes place outside the pump pulse amplification window. However, the pump laser suitable for a uOPA is demanding in terms of beam quality, energy stability and pulse duration, and therefore such system comes at the cost of an increase of system complexity.

Ideally, the temporally ultraclean amplifier modules developed for ultrahigh intensity lasers should deliver enough energy to replace the first amplification stage of a CPA laser system, which is typically in the 1-to-10 mJ energy range. Unfortunately, the energy available after an XPW-cleaning stage has been limited to few 100 µJ [12]. This is due to the nonlinear cleaning stage that is not scalable to higher energies in its current design, without increasing the footprint of the module dramatically. For the uOPA design, the highest energy has been demonstrated at PHELIX [13] in the 100 µJ range, ten years ago [11]. While picosecond OPA is fully scalable to the millijoule range given the aperture available in nonlinear crystals, a millijoule-level uOPA at PHELIX has not been demonstrated due to the lack of an available pump laser.

In this paper, we present a CPA laser developed at GSI-Darmstadt, Germany, as a self-seeded pump source for a millijoule-level ultrafast OPA in the spectral range 1000 - 1060 nm. To reach this goal, the amplifier has to provide an energy in excess of 100 mJ before compression and frequency conversion, which is achieved by a diode-pumped Yb:YAG regenerative main amplifier. Yb:YAG was chosen because of its energy storage capability and emission cross section bandwidth capable of supporting picosecond-pulse amplification. Nonetheless, the small gain bandwidth of Yb:YAG demands the employment of a self-phase-modulation (SPM) module before the pulse stretcher to enable self-seedability for a broader range of seed oscillators. This SPM-stage makes it a universal OPA pump laser for any ytterbium and neodymium-doped amplifier.

So far, two laser systems have been built, one to upgrade the Nd:glass laser PHELIX at GSI Hemholtzzentrum für Schwerionenforschung, in Darmstadt, Germany, and a second for the Yb:CaF_2 based PEnELOPE laser system at the Helmholtz Zentrum Dresden Rossendorf, Germany [14].

In the following, the first part of the article details the overall laser architecture and justifies the design in view of the desired performances. The second part describes the demonstrated performance of the laser system, knowing that two systems have been already built and extensively tested for reliability over a time span of 12 months.

2. Amplifier design

As pump source for a 1 mJ uOPA, the amplifier is strictly tied to several requirements. First of all, considerations must be made with regard to the pulse duration. Since uOPA is a process gated in time by the pump pulse, the pulse duration should not be too close to that of the signal pulse in order to reduce energy fluctuation due to potential temporal jitter. Nevertheless, the pulse duration should not be too long either, as this will reduce the efficiency of the process. Therefore, a pump pulse duration of 1 to 2 ps is targeted, which is sufficiently short to directly amplify pulses from most short-pulse oscillators. Although the pulse duration itself is of significant importance, it must be noted that the temporal contrast of the pump pulse plays a rather insignificant role, since the gain drops rapidly with decreasing intensity, making amplified spontaneous emission (ASE) and pre- or post-pulses in the pump profile unproblematic. On the contrary, the quality of the beam profile is a key factor for the uOPA process, since at high gain the beam profile of the pump is imprinted onto that of the signal. Last, the delivered energy of the pump pulse should factor in an energy budget, which allows to define a reliable operating point and make the system less susceptible to performance degradation. Estimates performed with the simulation code Miró

Optics EXPRESS

[15] at 'Ecole Polytechnique, France, call for a pump energy around 20 to 30 mJ at the uOPA stage, in order to reach reliably 1-mJ OPA output energy. Hence, we aim at an output energy of 100 mJ prior to compression and SHG.

Apart from these requirements, which are more specific to the uOPA process itself, three more points have to be discussed: repetition rate of the system, pump energy stability and its applicability in various laser systems. Concerning the former, our aim lies clearly in designing an amplifier that is compact and easy to maintain rather than trying to reach the highest average output powers. Although a tendency to higher repetition rates in ultra-short, high-energy lasers in the 100 J class is visible, most high-repetition rate high-energy systems perform in the range from 1 Hz to one shot every few minutes. Therefore, the proposed system is not designed to work in the kHz range but rather in the range of 10 Hz.

A second requirement imposed upon the pump laser by its use as a pump for driving nonlinear amplification processes is an enhanced energy stability requirement. As a consequence, laser-diode pumped amplifier materials are favored. Finally, the applicability in different laser systems and thus the seed acceptance of the system with pulses of the same oscillator should be considered. This self-seeding allows a first-order time synchronization between pump and signal pulse but is bound to the fact that a spectral overlap between the gain bandwidth of the pump amplifier and the spectrum of the signal is needed. For this application we aim at compatibility with oscillators working in the range of 1000 nm to 1060 nm, which addresses high-intensity lasers based on either Nd:glass or ytterbium-doped materials.

To account for all the above-mentioned requirements, we developed an ytterbium-based, two-stage chirped pulse amplifier consisting of a fiber module that combines seed generation, stretching and pre-amplification in an all-fiber setup followed by a regenerative main amplifier and a grating compressor. The schematic for the whole setup can be seen in Fig. 1.

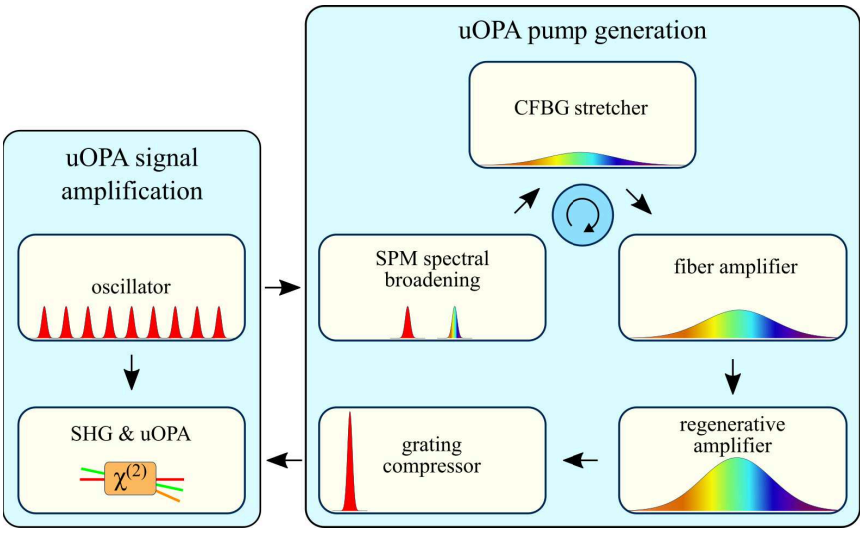

Fig. 1. Schematic drawing of the uOPA setup. The whole setup of the uOPA is split into two parts: a signal and a pump-amplification stage which are both seeded by the same laser oscillator. The pulses of the pump-amplification chain are first coupled into an SPM-stage before being stretched in a chirped fiber Bragg grating (CFBG) and propagating into a fiber pre-amplifier. Further amplification is done by a regenerative amplifier before the pulses are recompressed in a grating compressor. In a last step, the second harmonic of the pump pulse is created and sent to the uOPA stages.

Optics EXPRESS

The starting point of the signal and pump-amplification chain of the uOPA system is the short-pulse oscillator of the laser system. Due to the delay caused by the amplification time in the pump laser, temporally separated pulses of the pulse train are used to seed the uOPA and the pump system. As the oscillator delivers a sufficient amount of energy per pulse, the pulse train is not split in time but intensity-wise into two parts via half-wave plate (WP) and polarizer. The main part of the pulses' energy is used as seed for the uOPA amplification chain and a minimal part, as seed for the pump-amplification chain. The exact splitting ratio depends on the type of laser oscillator and its output pulse energy. The reason for this is quite clear, when thinking about how the self-seeding stage is implemented. While every oscillator that produces pulses with spectral overlap to the wavelength of Yb:YAG, corresponding to 1030 nm, is already ready to use as seed for the pump, a little more effort needs to be put in when there is no overlap. If one does not want to be limited to only these kinds of oscillators, the output spectra of other oscillators have to be manipulated to bridge a potential spectral gap. A simple, yet stable, solution to overcome this gap is realized by using spectral broadening via SPM in a common polarization-maintaining-fused-silica fiber prior to the stretcher of the CPA.

In our case a fiber with a mode field diameter of 6.6 µm (Corning, PANDA PM980) is used. Thanks to the domination of the nonlinear Kerr-effect over the dispersion within the first few centimeters of propagation inside the fiber, the spectrum can sufficiently broaden to overlap with the spectral range of a Yb:YAG amplifier. For even more drastically broadened spectra an exchange of this common fiber by a more specialized nonlinear fiber (e.g., highly nonlinear photonic crystal fibers) could be conducted, which would enable compatibility to a wider range of oscillators with the presented pump amplifier. However, for the sake of simplicity and maintainability our setup works with the standard PANDA fibers which are easily spliceable to a circulator (C in Fig. 2) (AFR, HPMCIR-03-0.3-S-S-Q-C(SR13739B)). The circulator connects the input with the stretcher of the system which employs a CFBG (TeraXion, PowerSpectrum HPSR). The CFBG reflects a bandwidth of 3.75 nm centered around 1030 nm while stretching it to 1.2 ns pulse duration, corresponding to a stretching factor of 320 ps/nm. The stretching factor of the system has been chosen to be large enough to mitigate further nonlinear effects in the amplifiers, but also to be small enough to enable a reasonably compact design for the compressor of the CPA.

After stretching the pulse is fed into the fiber-amplifier stages. The first one consists of an Yb-doped single mode, single cladding and polarization maintaining fiber (Coherent, PM-YSF-HI-HP) with a length of 1.3 m that is pumped by a continuous wave, single-mode laser diode (LD) (3SPTechnologies, RLS/976NM-750MW) at 976 nm in a co-propagating fashion. The combining of these two beams is realized via wavelength division multiplexing (WDM) (AFR, PMFWDM-9703-N-B-Q). To protect the oscillator from potential backward propagating light, a Faraday isolator (FI) (AFR,HPMI-03-A-0.1-N-B-Q-F-1-C) is installed.

Prior to further amplification a reduction of the repetition rate of the pulse train down to 100 kHz is conducted via fiber coupled Acousto-Optic-Modulator (AOM) (G&H, FiberQ T-M300-0.1C2G-3-F2P). This allows the energy of the individual pulses to be increased, since the available pump power is distributed over a reduced number of pulses. From this point on, the output is fed through a fiber coupled FI (AFR, HPMI-03-A-10-N-B-Q-F-1-P) into the second fiber-amplifier stage. The latter is a 1.55 m long Yb-doped, double-clad, photonic-crystal fiber (PCF) with a large mode-area (LMA) with a diameter of 15 µm (NKT-Photonics, DC-135/14-PM-Yb) pumped at 976 nm in a counter-propagating setup by a fiber-coupled, multi-mode LD (PhotonTec, M976±0.5-7-F105/22-G4T). In addition, three monitor outputs (Mon in Fig. 2) are installed that allow to check the performance of the system or diagnose malfunctions. The whole fiber-setup is shown in Fig. 2.

After pre-amplification, the output of the fiber-module feeds the main amplifier to boost the energy up to the targeted energies in the range of 100 mJ. A schematic drawing of this amplifier

Optics EXPRESS

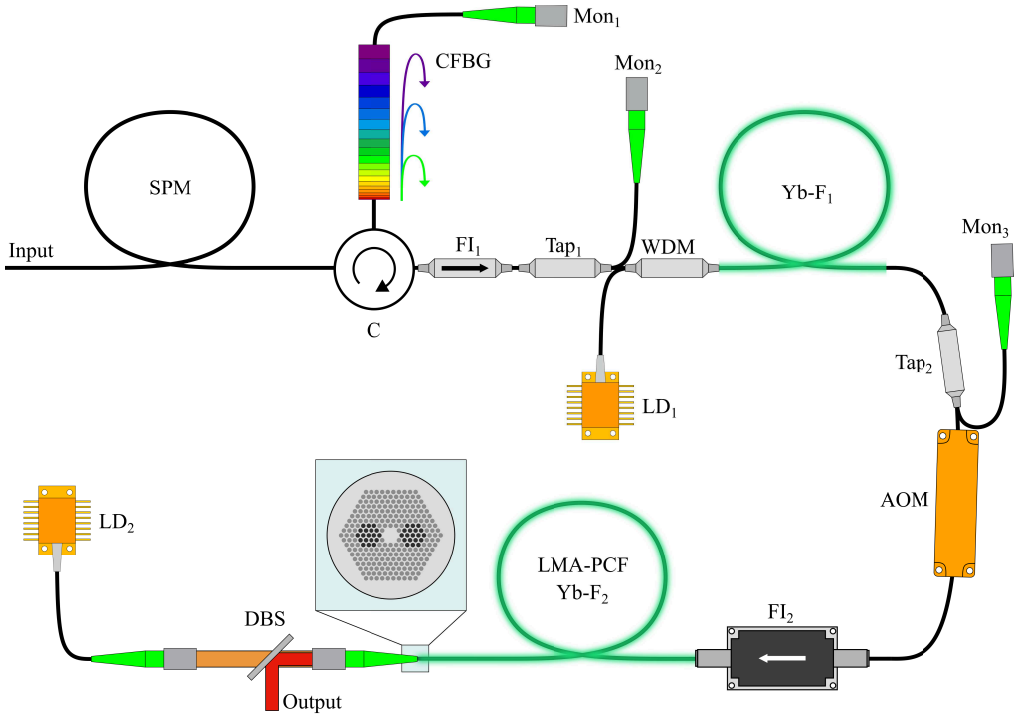

SPM:	Self-Phase-Modulation	Yb-F:	Yttberium doped fiber
C:	Circulator	LD:	Laser Diode
CFBG:	Chirped Fiber Bragg Grating:	AOM:	Acousto-Optic Modulator
Mon:	Monitor Output	LMA:	Large Mode Area
FI:	Faraday Isolator	PCF:	Photonic Crystal Fiber
Tap:	Tap/Coupler	DBS:	Dichroic Beam Splitter
WDM:	Wavelength Division Multiplexer		

Fig. 2. Schematic drawing of the fiber stage. This stage combines the spectral broadening of the seed, the stretcher and the pre-amplifier of the CPA in a whole-fiber-system. The amplification is done in laser-diode pumped Yb-doped fibers, split in two distinct stages that are coupled via AOM.

can be seen in Fig. 3. For optimized coupling between the fiber pre-amplifier and the regenerative main amplifier a three-lens, mode-matching telescope is set up. Since the main amplifier is designed as a linear cavity for reasons of compactness and simplicity, further safety measures have to be applied to protect the delicate fiber-stage output from backward-propagating energetic leakage pulses. Therefore, a set of two FIs and a Faraday rotator (FR) (Coherent, Pavos series) are set up in between the two amplifiers. In the next step, the pulses pass a motorized delay stage (DS_1), which is used for the long-term stabilization of the temporal overlap between pump and signal in the uOPA process. Finally, a polarizer (Pol_1) and a half-wave retardation Pockels cell (PC $\lambda/2$) (Leysop, EM510M), used as a pulse picker, build the main separation-module for the in- and outgoing pulses. With this, every 10000th pulse is transmitted through the cavity-polarizer (Pol_2), while the rest is reflected and dumped. The cavity itself consists of two curved end mirrors (r=-20 m - VexM and r=15 m - CavM), a 20 mm long PC, a quarter WP, two folding mirrors to reduce the amplifier footprint and a single Yb:YAG crystal.

With the chosen mirror radii and a distance of approximately 1.7 m in between, the beam radius of the bare cavity changes only slowly from a minimum of 1.6 mm to a maximum of

Optics EXPRESS

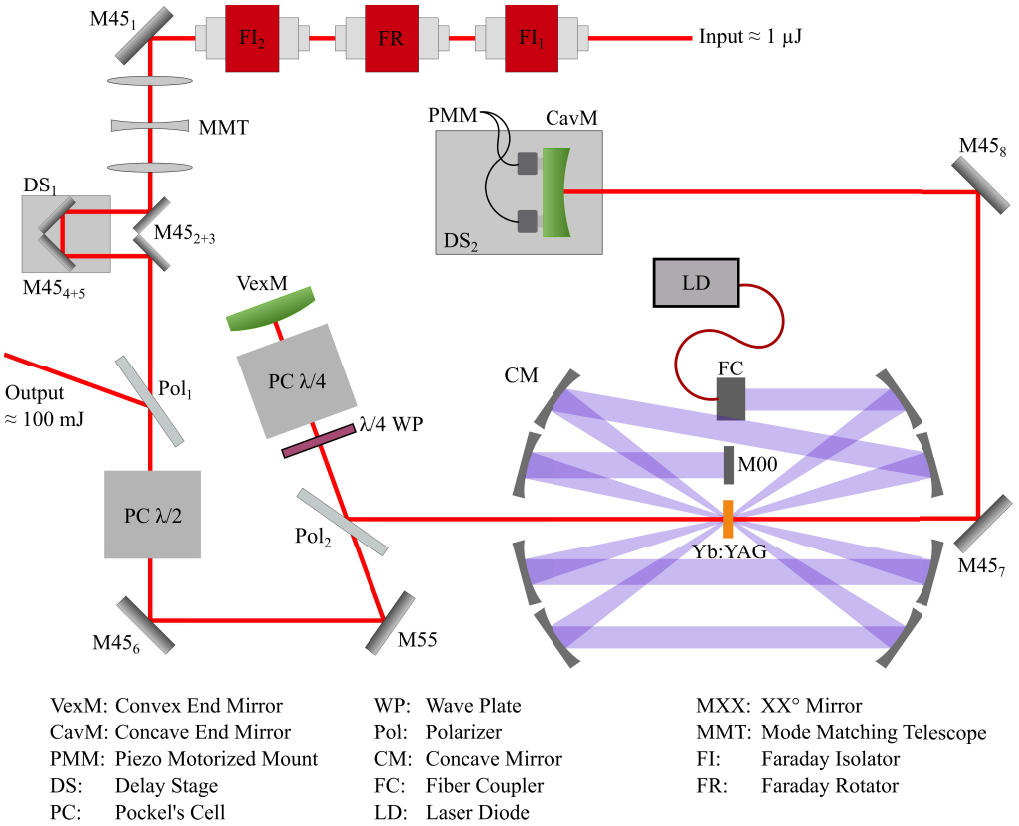

Fig. 3. Schematic drawing of the regenerative main amplifier and its input setup. The cavity is built around a single Yb:YAG crystal, pumped by a 12-pass pump system (for reasons of clarity only eight passes are drawn), powered by a fiber-coupled, high-power LD. A single PC, WP and pair of curved mirrors are used to set up a stable, regenerating cavity.

1.8 mm without having a waist inside the cavity. Nonetheless, since high fluences are expected, the thicknesses of transmissive optics are kept as low as possible to keep nonlinear effects at a minimum. Therefore, the active medium is a 1 mm thick, 5 % doped Yb:YAG crystal with a diameter of 12 mm mounted to a ring-shaped, cooled, copper heat sink, that is set up in the center of a 12-pass pump scheme and as close as possible to the PC, which, because it accounts for 93 % of the optical path length inside media, is the major contributor to self-focusing. Since the system operates at 10 Hz, it is less prone to thermal effects.

Here, the output of a high-power, fiber-coupled LD (Coherent, M1F4S22-940.3-1000Q) with a central wavelength of 940 nm and pulse energies up to 1.1 J is sent through the crystal. For enhanced absorption, the crystal is hit 12 times. To maintain the smooth profile of the pump beam at the output of the 400-µm multi-mode fiber, the pump mirrors (CM in Fig. 3) inhibit a concave surface with a radius of 30 cm and build a set of 4-f telescopes to image the pump profile at the crystal position onto itself. With a focal length of 2.5 cm of the initial collimating lens inside the fiber coupler (FC), a six-fold magnification of the fiber output to a pump spot of 2.4 mm is realized. Lastly, two remotely controllable, mechanical elements are installed. For the alignment of the cavity during the warm-up time and to not disturb the environment of the housed cavity, the tip- and tilt-axes of the CavM are controllable via piezo-motors (PMM in Fig. 3). Additionally, the mirror is mounted on a motorized DS with 5 cm travel range.

Optics EXPRESS

While this travel distance only has a negligible influence on the mode size, below 1 %, the impact of this stage is of relevance concerning the use of this amplifier in terms of a uOPA pump. Since a precise temporal overlap between pump and seed is needed within the uOPA process, it is often useful to be able to bridge a gap of a few nanoseconds due to typical oscillator repetition rates around 80 MHz. This coarse synchronization between pump and seed pulses is easily achieved here, since every displacement of the motorized stage is multiplied by the number of roundtrips, hence covering meter-scale optical path difference with only a few centimeters of mirror translation. In our implementation, the 5-cm travel distance of the motorized stage enables a temporal shift of the pump pulse of 8.3 ns for a regenerative amplification of 50 roundtrips, which is enough to match temporally the seed pulse from oscillators with repetition rates as low as 60 MHz.

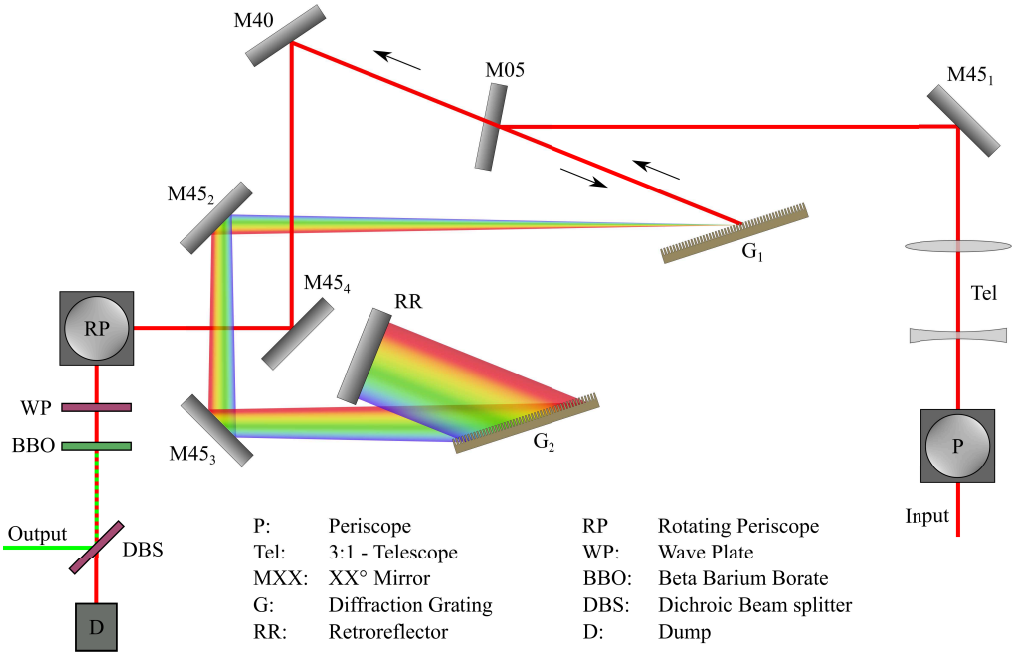

Fig. 4. Schematic drawing of the compressor. A simple Treacy compressor is folded to increase the compactness of the system.

Finally, the last part of the laser consists of the pulse compressor, which is a standard Treacy-type reflective-grating compressor. The dispersion of this matches that of the CFBG, such that most of the spectral phase orders can be compensated. Hence, the perpendicular distance between the gratings G_1 and G_2 of 342.8 mm, combined with an incidence angle of 62.3° results in an overall distance of 1.2 m between the gratings. To account for a compact setup, the compressor is folded using two folding mirrors in the spectral dispersed domain (see Fig. 4). The spatial separation after a double pass in the compressor is managed via a retroreflecting mirror (RR) that introduces a vertical displacement of 2 cm. The gratings themselves are 50 mm x 50 mm clear aperture multilayer- dielectric gratings with a line density of 1790 l/mm on a 60 mm x 60 mm fused silica substrate (Plymouth Grating Laboratory, PGL3751-FB).

Optics EXPRESS

3. Performance of the CPA pump system

3.1. Seed generation and fiber pre-amplifier

As described in the design section, one of the key features of the pump system is its capability to work with the seed of different oscillators at different wavelengths. Since at least two distinct laser systems, namely PHELIX and PENELOPE, will use this pump laser, compatibility with their two different laser oscillators has to be ensured.

The short-pulse source at PENELOPE is a commercial, passively mode-locked Yb-based oscillator (Light Conversion, Flint) running at a central wavelength of 1034 nm, with a bandwidth of 25 nm FWHM (see Fig. 5(a)) and a transform limited pulse duration below 65 fs, making it a suitable choice to seed the PENELOPE pre and main amplifiers based on Yb:CaF_2 as gain material. With a repetition rate of 78 MHz and a quasi-CW output power of about 900 mW, the pulse energy is in the range of 11.5 nJ, which is easily splittable to seed the uOPA pump and signal chain. Since its spectrum already covers the needed range for the uOPA pump system its compatibility is ensured even without SPM-stage.

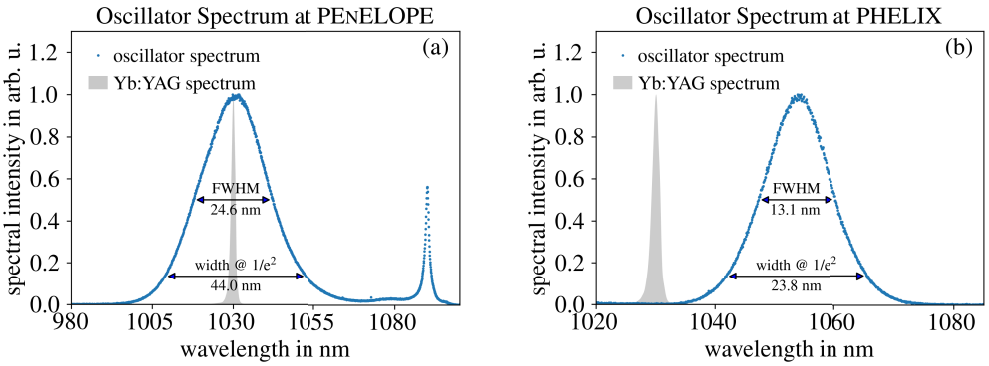

Fig. 5. Comparison of the spectra of the short-pulse oscillators at PENELOPE (a) and PHELIX (b). While the spectrum in (a) can unproblematically seed a Yb:YAG laser (a typical spectrum is indicated as gray area), some extra measures have to be taken for the spectrum in (b) to overcome the spectral gap.

Due to PHELIX' rod pre-amplifier and slab main-amplifier consisting of Nd:glass, the pulse source, which is a passively mode-locked Ti-sapphire based oscillator (Coherent, Mira Optima 900-F), is tuned to a central wavelength of 1054 nm (see Fig. 5(b)) to ensure efficient seeding of its pre and main amplifiers. The outgoing pulse train features 3 nJ pulses at a repetition rate of 72 MHz with a spectral bandwidth of 13 nm FWHM centered at 1054 nm and a pulse duration below 115 fs. As can be seen in Fig. 5(b) the spectral bandwidth of the oscillator is not sufficient to be used as seed for a Yb:YAG amplifier. Hence, the spectral broadening via SPM is mandatory to seed the pump laser.

In Fig. 6 the input and outcome of the SPM-stage after injecting pulses of the PHELIX oscillator can be seen. The 13 nm broad input spectrum centered around 1054 nm (blue curve, Fig. 6(b)) is broadened to 37 nm (orange curve, Fig. 6(b)). Although further broadening would be possible, the least amount has been chosen that suffices to seed the fiber amplifier to mitigate further nonlinear interactions. The resulting spectrum after being stretched by the CFBG can be seen in Fig. 6(a). From 70 mW seed before coupling into the fiber-system, 2 mW, corresponding to about 30 pJ per pulse remain as effective input seed power for the fiber amplifier. Within the two-stage fiber system the pulses are amplified with a gain factor of approximately 10^5. In comparison to our previous work [16], the 'all-fiber-system' enables a more efficient coupling between the two amplification stages. Hence, the system enabled tuning the repetition rate of

Optics EXPRESS

the second fiber stage because of the enhanced input power. In Fig. 7 the output characteristics, namely the pulse energy and pulse spectrum are shown.

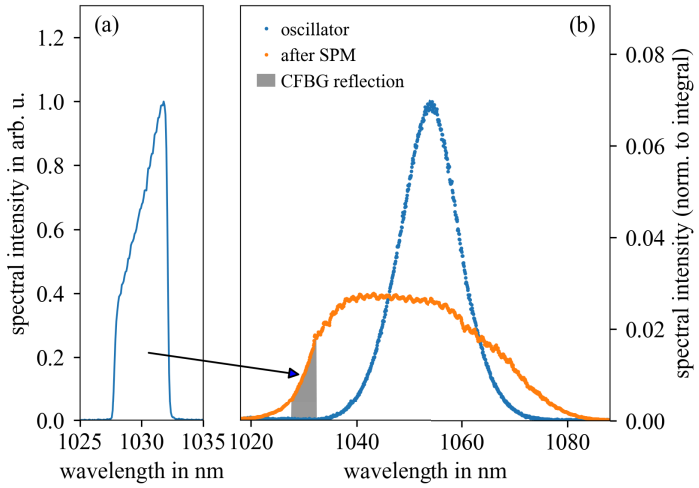

Fig. 6. Demonstration of the SPM-stage at the PHELIX laser. The spectrum of the input pulse (b, blue) is sufficiently broadened (b, orange) to seed the fiber amplification stage. The stretched part of the spectrum is depicted on the left side (a).

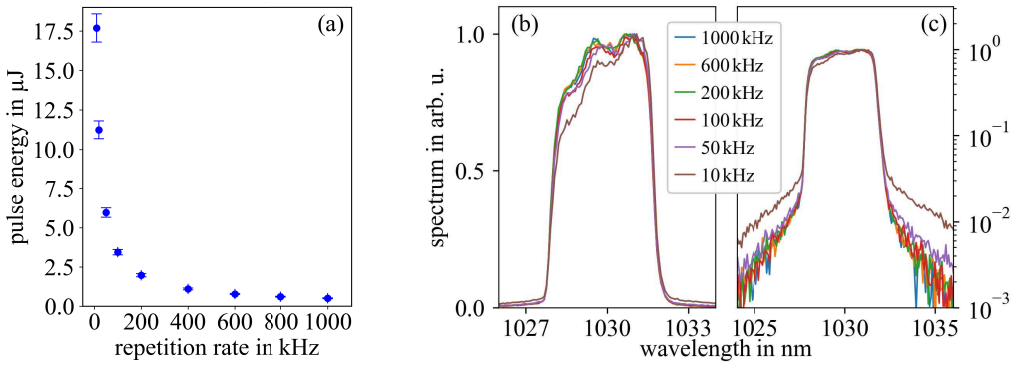

Fig. 7. (a): Increase of the fiber pre-amplifier output energy by tuning of the repetition rate. (b)/(c): Comparison of the spectra after pre-amplification at different repetition rates. (b): linear scale, (c): log-scale.

In Fig. 7(a), the output energy increases significantly with reduced repetition rate of the second fiber stage, going up to 17.5 µJ which represents an energy increase of 35 compared to the 1 MHz repetition rate. Although, this energy increase seems beneficial, one must watch out for unwanted effects such as the Kerr effect and ASE. Concerning the Kerr effect, problems may occur when going to even higher energies. However, at 17.5 µJ the nonlinear length [17] is already as low as 4.5 cm and small effects are expected. Moreover, when having a look at the output spectra (Fig. 7(b), (c)), distorting of the spectral distribution starting at 50 kHz and a slight increase of ASE in the wings of the plot is visible. For this reason, the working point of the second stage has been set to 100 kHz, delivering seed pulses for the regenerative main amplifier with energies of (3.4 ± 0.2) µJ where the inaccuracy is dominated by the systematic error of the power meter.

Optics EXPRESS

3.2. Regenerative main amplifier and pulse compression

Inside the main amplifier these pulses are amplified to a maximum energy of 108 mJ. This limit is mainly set by the onset of nonlinear effects and their impact on the spatial mode of the cavity. This can be seen on the plot in Fig. 8(a). As the output energy increases, two consequences of the Kerr effect can be observed. First, the SPM manifests by increasing the spectral bandwidth by 0.35 nm or roughly one third of its total bandwidth when turning up the signal output from 14 mJ to 108 mJ (blue points). Second, the beam radius decreases as a consequence of Kerr-induced self-focusing inside the transmissive optics, where the main influence is estimated to originate in the 20-mm-long PC. Despite the nonlinear self-focusing, a stable mode is formed in the cavity, whose intensity distribution can be seen in Fig. 9(b).

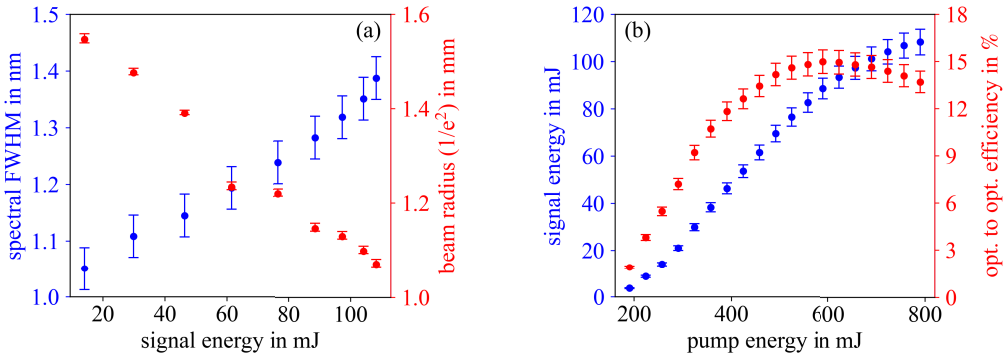

Fig. 8. (a): Spectral FWHM and beam radius in dependency of the output energy. The y-axes are color-coded to match the represented data. The beam profile has been measured outside the cavity in 65 cm distance to the cavity output. (b): Output energies and optical to optical efficiency in dependency of the input pump energy.

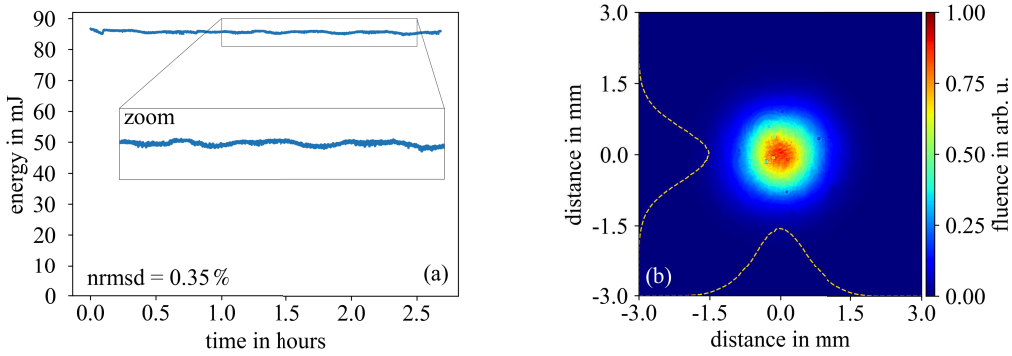

Fig. 9. (a): Energy stability of the regenerative amplifier for roughly 3 hours without interaction. The inlet shows a close-up of the energy fluctuation induced by the air conditioning system. (b): Output beam profile of the main amplifier at 108 mJ energy, recorded 65 cm after the cavity output through a leakage mirror outside the cavity.

As shown in Fig. 8(b), the output of the cavity scales nearly linearly with the used pump energy up to the point of maximum optical to optical efficiency (ratio of signal-output energy to pump-input energy) of 15 % at an output energy of 90 mJ. When further increasing the pump energy, the output energy increases, but with reduced efficiency due to a smaller mode and

Optics EXPRESS

decreased gain inside the active medium. At the point of optimum efficiency the build-up time to saturation takes only 288 ns, corresponding to a total roundtrip number of 25.

Fig. 9(a) illustrates the energy output stability of the main amplifier. After a short warm-up time of 6 min, the signal stabilizes and remains stable over many hours. The energy stability reaches then 0.35 %, mostly dominated by slow energy drifts. We identified the origin of these oscillations being the air conditioning system in the test laboratory that is not optimized to perfectly maintain the temperature, but periodically only cools the room to a specified temperature. Concerning the beam quality an M^2 measurement, using an f = 1 m lens, after the compression of the pulses has been conducted. The measured beam sizes and the corresponding fit can be seen in Fig. 10(a). As the measurement shows, the beam inhibits a slight astigmatism and a different beam quality for the x- and y-axis. While the beam quality in the x-axis is close to the ideal with an $M_x^2 = 1.02 \pm 0.02$, the beam quality of the y-axis is in the range of $M_y^2 = 1.16 \pm 0.04$. A potential reason for the differences in beam quality may be the trapezoidal shape in x-direction of the PC (0.5° wedge on each side) inside the cavity that causes asymmetric refraction between the two axes. Due to a rotating periscope (RP in Fig. 4) at the output of the compressor, this of course translates to effects in the y axis. The compressor as origin for the beam quality difference can be omitted since an M^2 measurement prior to compression showed no difference to a measurement after compression. In Fig. 10(b), the focal spot at the position of smallest beam diameter of the y-axis can be seen. The compressor itself features a total transmission of (85.6 ± 0.8) %, meaning 92 mJ at full energy. This is slightly lower than one would expect from the measured grating efficiency alone, which was characterized above 98 %. By careful inspection of the transmitted spectra through the compressor, we could identify spectral clipping at G_2 as the main reason for the reduced transmission efficiency. This is of course improvable but does not impose problems as long as the pulse can be sufficiently compressed. The associated pulse durations, measured with a home-built SHG-FROG, are shown in Fig. 11 for two different output energies of the regenerative amplifier at the same number of roundtrips: 80 mJ (Fig. 11(a)) and 100 mJ (Fig. 11(b)). As one can see, the pulse is nicely compressible up to a certain energy. Quantitative measures like the FWHM show a near perfect compression when compared to the FTL with (1.27 ± 0.03) ps measured and (1.21 ± 0.01) ps FTL for 80 mJ and (1.38 ± 0.04) ps measured and (1.27 ± 0.02) ps FTL for 100 mJ. However, when comparing the shapes of the pulses, clear differences are visible and a degradation of the pulse form when increasing the output energy from 80 mJ to 100 mJ is observable. This result fits to estimates of the B-Integral, which is 0.8 rad at 80 mJ and 1.25 rad at 100 mJ.

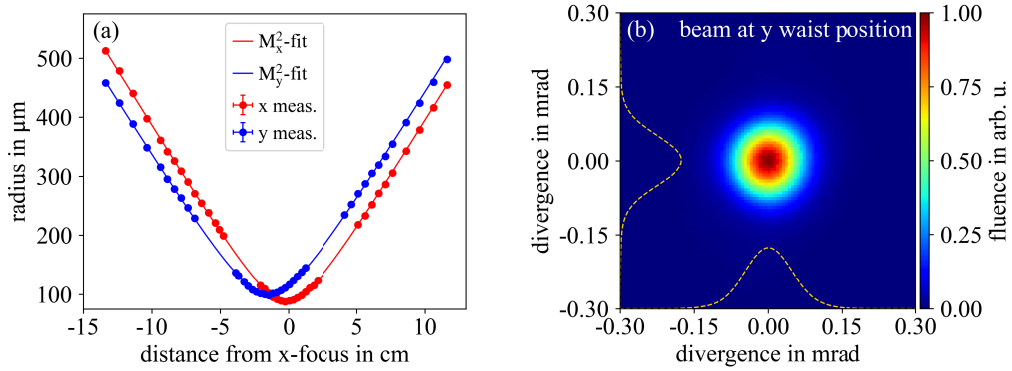

Fig. 10. (a): M^2 measurement after compression at maximum energy with a 1 m lens with $M_x^2 = 1.02 \pm 0.02$ and $M_y^2 = 1.16 \pm 0.04$. (b): Energy distribution of the beam at the focal-spot position of the y-axis. The dashed lines represent the sum over the axes in x and y, respectively.

Optics EXPRESS

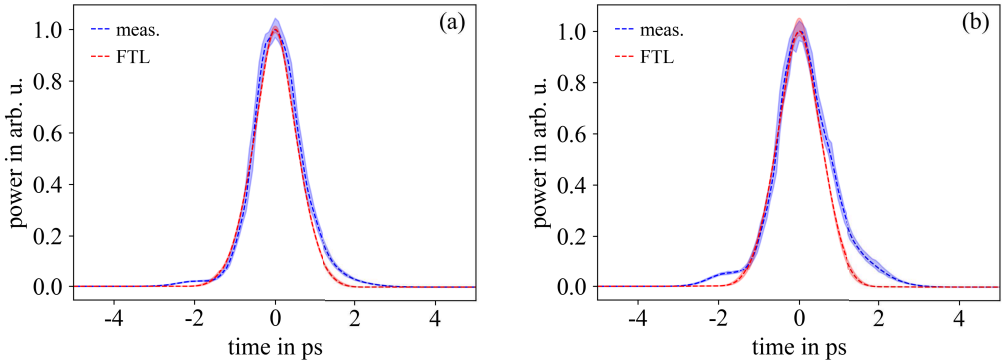

Fig. 11. Comparison of the compressed pulses at 80 mJ (a) and 100 mJ (b). The pulses, measured with an SHG-FROG, are depicted in blue with reconstruction errors (peak-to-valley) as blue shaded area. The Fourier transform limit (FTL) is shown in red.

Of course, this may translate into pulses with nonlinear-effect dominated spectral phases that are not perfectly compressible with a standard grating compressor. Therefore, the increase in peak power going from 80 mJ to 100 mJ is not as high as 25 % but still 13 %. Lastly, the compressed pulses are frequency doubled to 515 nm in an 0.6 mm thick beta Barium Borate (BBO) crystal for the later use as uOPA pump-pulses. In Fig. 12 the efficiency of the SHG-process in dependence of the input energy can be seen.

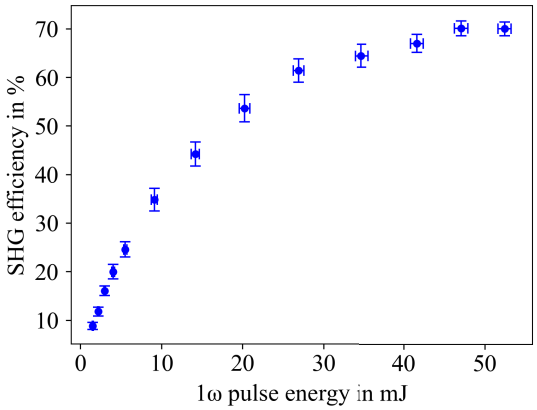

Fig. 12. SHG efficiency in dependency of the input pulse energy after compression.

The SHG efficiency starts to saturate already below 10 mJ of input energy and reaches a maximum value of (70.1 ± 1.5) % for input energies above 50 mJ. Due to damage thresholds of the frequency-doubling crystals and self-focusing after compression the current maximum energy at 2ω is 43 mJ.

4. Conclusion

We developed a CPA-type pump laser, based on ytterbium-doped gain media, for the use in uOPA applications that is capable of generating 108 mJ pulses pre-compression and 92 mJ pulses post-compression with pulse durations of (1.38 ± 0.04) ps (FWHM) at maximum energy. Thanks to a fiber-based pre-amplifier with a SPM module, this laser is usable for different kinds of oscillators at different wavelengths that initially may not possess bandwidth in the needed spectral

Optics EXPRESS

region, even for very little input seed energies, which allows to use the same seed source for the signal and pump of the uOPA, resulting in higher stability in terms of temporal synchronicity. In terms of energy stability, the system delivers pulses with an excellent energy stability of 0.35 %, at 10 Hz repetition rate, inhibiting an outstanding beam quality of $M_x^2 = 1.02 \pm 0.02$ and $M_y^2 = 1.16 \pm 0.04$. After compression an SHG efficiency of 70 % is achievable and a maximum energy of 43 mJ has been obtained. To further increase this energy, a larger beam size would be needed to prevent laser induced damage on the SHG crystal. Consequently, the SHG crystal and the width of the second compressor grating also need to be increased to minimize clipping losses. Nevertheless, compared to previous work from our group [11,16], this new laser delivers an order of magnitude more energy and incorporates several technical improvements, which enable reaching better beam quality and energy stability.

We believe that our system can be adapted to 800 nm wavelength oscillators without much additional work. To seed the 1030 nm amplifier with a 800 nm oscillator, the seed energy requirement will be higher than in our case, but still in reach of a >10 nJ Ti:sapphire oscillator (e.g. in [18]). Since a pump at 515 nm is capable of broadband phase matching even at these wavelengths, for example in a non-collinear BBO setup [19], we think that other laboratories, which work with Ti:sapphire oscillators, will also benefit from the implementation of our pump module.

The system is already in use and replaced the existing pump system for the uOPA at PHELIX, providing a stable and clean amplification process for high-contrast experiments. In the near future, this system will be also commissioned at the PEnELOPE laser system.

Funding. ATHENA project of the Helmholtz Association; European Union's Horizon 2020 research and innovation programme under grant agreement no. 871124 Laserlab-Europe; HMWK of the state of Hesse through the LOEWE center "Nuclear Photonics".

Acknowledgments. The authors thank Dr. Ji-Ping Zou from École Polytechnique, France, for her input and support through Miró calculations.

Disclosures. The authors declare no conflicts of interest.

Data availability. Data underlying the results presented in this paper are not publicly available at this time but may be obtained from the authors upon reasonable request.

References

1. D. Strickland and G. Mourou, "Compression of Amplified Chirped Optical Pulses," Opt. Commun. **56**(3), 219–221 (1985).
2. F. Wagner, S. Bedacht, A. Ortner, M. Roth, A. Tauschwitz, B. Zielbauer, and V. Bagnoud, "Pre-plasma formation in experiments using petawatt lasers," Opt. Express **22**(24), 29505–29514 (2014).
3. J. W. Yoon, Y. G. Kim, I. W. Choi, J. H. Sung, H. W. Lee, S. K. Lee, and C. H. Nam, "Realization of laser intensity over 10 23 W/cm 2," Optica **8**(5), 630–635 (2021).
4. A. Jullien, O. Albert, F. Burgy, G. Hamoniaux, J.-P. Rousseau, J.-P. Chambaret, F. Augé-Rochereau, G. Chériaux, J. Etchepare, N. Minkovski, and S. M. Saltiel, "10^10 Temporal Contrast for Femtosecond Ultraintense Lasers By Cross-Polarized Wave Generation," Opt. Lett. **30**(8), 920–922 (2005).
5. M. P. Kalashnikov, E. Risse, H. Schönnagel, and W. Sandner, "Double chirped-pulse-amplification laser: a way to clean pulses temporally," Opt. Lett. **30**(8), 923–925 (2005).
6. B. Dromey, S. Kar, M. Zepf, and P. Foster, "The plasma mirror - A subpicosecond optical switch for ultrahigh power lasers," Rev. Sci. Instrum. **75**(3), 645–649 (2004).
7. G. Doumy, F. Quéré, O. Gobert, M. Perdrix, P. Martin, P. Audebert, J. C. Gauthier, J. P. Geindre, and T. Wittmann, "Complete characterization of a plasma mirror for the production of high-contrast ultraintense laser pulses," Phys. Rev. E **69**(2), 026402 (2004).
8. A. Lévy, T. Ceccotti, P. D'Oliveira, F. Réau, M. Perdrix, F. Quéré, P. Monot, M. Bougeard, H. Lagadec, P. Martin, J.-P. Geindre, and P. Audebert, "Double plasma mirror for ultrahigh temporal contrast ultraintense laser pulses," Opt. Lett. **32**(3), 310–312 (2007).
9. C. Thaury, F. Quéré, J. P. Geindre, A. Levy, T. Ceccotti, P. Monot, M. Bougeard, F. Réau, P. D'Oliveira, P. Audebert, R. Marjoribanks, and P. Martin, "Plasma mirrors for ultrahigh-intensity optics," Nat. Phys. **3**(6), 424–429 (2007).
10. C. Dorrer, I. A. Begishev, A. V. Okishev, and J. D. Zuegel, "High-contrast optical-parametric amplifier as a front end of high-power laser systems," Opt. Lett. **32**(15), 2143 (2007).

Optics EXPRESS

11. F. Wagner, C. P. Jo ao, J. Fils, T. Gottschall, J. Hein, J. Körner, J. Limpert, M. Roth, T. Stöhlker, and V. Bagnoud, "Temporal contrast control at the PHELIX petawatt laser facility by means of tunable sub-picosecond optical parametric amplification," Appl. Phys. B **116**(2), 429–435 (2014).
12. L. P. Ramirez, D. N. Papadopoulos, A. Pellegrina, P. Georges, F. Druon, P. Monot, A. Ricci, A. Jullien, X. Chen, J. P. Rousseau, Y. Liu, A. Houard, and R. Lopez-Martens, "High energy and efficient cross polarized wave generation for high contrast ultrashort laser sources," Opt. InfoBase Conf. Pap. **19**, 93–98 (2011).
13. V. Bagnoud, B. Aurand, A. Blazevic, S. Borneis, C. Bruske, B. Ecker, U. Eisenbarth, J. Fils, A. Frank, E. Gaul, S. Goette, C. Haefner, T. Hahn, K. Harres, H. M. Heuck, D. Hochhaus, D. H. Hoffmann, D. Javorková, H. J. Kluge, T. Kuehl, S. Kunzer, M. Kreutz, T. Merz-Mantwill, P. Neumayer, E. Onkels, D. Reemts, O. Rosmej, M. Roth, T. Stoehlker, A. Tauschwitz, B. Zielbauer, D. Zimmer, and K. Witte, "Commissioning and early experiments of the PHELIX facility," Appl. Phys. B **100**(1), 137–150 (2010).
14. M. Siebold, F. Roeser, M. Loeser, D. Albach, and U. Schramm, "PEnELOPE: a high peak-power diode-pumped laser system for laser-plasma experiments," High-power, high-energy, high-intensity laser technol. res. using extrem. light enter. new front. with petawatt-class lasers **8780**, 1–14 (2013).
15. O. Morice, "Miró: Complete modeling and software for pulse amplification and propagation in high-power laser systems," Opt. Eng. **42**(6), 1530–1541 (2003).
16. C. P. João, F. Wagner, J. Körner, J. Hein, T. Gottschall, J. Limpert, and V. Bagnoud, "A 10-mJ-level compact CPA system based on Yb:KGW for ultrafast optical parametric amplifier pumping," Appl. Phys. B **118**(3), 401–407 (2015).
17. G. P. Agrawal, *Nonlinear fiber optics* (Academic University, 2001), 3rd ed.
18. Newport Corporation, Tsunami ® Series - Ti:Sapphire Ultrafast Oscillators, (2021).
19. C. Manzoni and G. Cerullo, "Design criteria for ultrafast optical parametric amplifiers," J. Opt. **18**(10), 103501 (2016).